Subcompartments of the macrophage recycling endosome direct the differential secretion of IL-6 and TNFα

Anthony P. Manderson, Jason G. Kay, Luke A. Hammond, Darren L. Brown, and Jennifer L. Stow

Institute for Molecular Bioscience, The University of Queensland, Brisbane QLD 4072, Australia

Activated macrophages secrete an array of proinflammatory cytokines, including tumor necrosis factor-α (TNFα) and interleukin 6 (IL-6), that are temporally secreted for sequential roles in inflammation. We have previously characterized aspects of the intracellular trafficking of membrane-bound TNFα and its delivery to the cell surface at the site of phagocytic cups for secretion (Murray, R.Z., J.G. Kay, D.G. Sangermani, and J.L. Stow. 2005. *Science*. 310:1492–1495). The trafficking pathway and surface delivery of IL-6, a soluble cytokine, were studied here using approaches such as live cell imaging of fluorescently tagged IL-6 and immunoelectron microscopy. Newly synthesized IL-6 accumulates in the Golgi complex and exits in tubulovesicular carriers either as the sole labeled cargo or together with TNFα, utilizing specific soluble NSF attachment protein receptor (SNARE) proteins to fuse with the recycling endosome. Within recycling endosomes, we demonstrate the compartmentalization of cargo proteins, wherein IL-6 is dynamically segregated from TNFα and from surface recycling transferrin. Thereafter, these cytokines are independently secreted, with TNFα delivered to phagocytic cups but not IL-6. Therefore, the recycling endosome has a central role in orchestrating the differential secretion of cytokines during inflammation.

Introduction

A key function of activated macrophages is to secrete cytokines, releasing these mediators in a tightly orchestrated manner to regulate the progression of an inflammatory response. The rapid production and secretion of TNFα by macrophages in response to microbial stimuli is central to induction of the early stages of inflammation, especially the recruitment of neutrophils. In addition to the protective role of TNFα during acute inflammatory responses, the overproduction or prolonged secretion of TNFα underlies the pathology of several chronic diseases, such as rheumatoid arthritis, graft-versus-host disease, and Crohn's disease (Beutler, 1999). For this reason, TNFα is the target of drugs and therapeutic antibodies, which are now increasingly used to treat these chronic inflammatory conditions (Siddiqui and Scott, 2005). Knowledge of the intracellular pathways responsible for TNFα trafficking and secretion could further aid drug development in this field. To this end, we recently defined the route for biosynthetic trafficking of membrane-bound TNFα and its release from activated macrophages (Pagan et al., 2003; Murray et al., 2005a,b; Kay et al., 2006). Newly synthesized TNFα rapidly accumulates in the Golgi complex upon the stimulation of macrophages with lipopolysaccharide (LPS) and is then transported to an intermediate compartment, the recycling endosome, before delivery to the plasma membrane for secretion.

A second proinflammatory cytokine produced by activated macrophages is interleukin 6 (IL-6), which, lacking a transmembrane domain, is trafficked and secreted directly as a soluble protein. IL-6 is produced somewhat later in the inflammatory response and is important in the early resolution phase of innate responses and in the induction of acquired immunity (Ulich et al., 1991; Barton and Jackson, 1993; Hurst et al., 2001; for review see Jones, 2005). The inappropriate or chronic production of IL-6 has also been implicated in several inflammatory diseases, in which it is often targeted, alone or in conjunction with TNFα, by drugs and antibodies (Nishimoto and Kishimoto, 2004). In activated macrophages, the expression and secretion profiles for TNFα and IL-6 generally overlap, although in a sequential fashion (Andersson and Matsuda, 1989; Kwak et al., 2000). Nothing is currently known about the intracellular trafficking of

Correspondence to Jennifer L. Stow: j.stow@imb.uq.edu.au

Abbreviations used in this paper: IL-6, interleukin 6; LPS, lipopolysaccharide; M6PR, mannose-6-phosphate receptor; Stx, syntaxin; Tfn, transferrin; TfnR, Tfn receptor; VAMP3, vesicle-associated membrane protein 3.

The online version of this article contains supplemental material.

The Journal of Cell Biology, Vol. 178, No. 1, July 2, 2007 57–69
http://www.jcb.org/cgi/doi/10.1083/jcb.200612131

IL-6. Therefore, the question begs as to whether soluble IL-6 is secreted via the same pathway as the membrane-bound TNFα and, furthermore, whether both cytokines rely on the same intracellular carriers and trafficking machinery.

In recent years, the combination of high resolution microscopy and live cell imaging of fluorescently tagged proteins has largely redefined the post-Golgi trafficking and sorting of biosynthetic cargo in polarized and nonpolarized cells. Importantly, these studies have demonstrated that biosynthetic cargo exits the TGN in pleomorphic, often tubular carriers that fuse with intermediate compartments in transit to the cell surface (Orzech et al., 2000; Ang et al., 2004; Lock and Stow, 2005; Murray et al., 2005a). All of the aforementioned studies implicate the recycling endosome as a way station for biosynthetic cargo and one wherein the cargo is likely sorted for transport to apical or basolateral membranes in polarized cells. The recycling endosome also, and more traditionally, handles cargo recycling from endosomal compartments to the cell surface, such as transferrin (Tfn) and Tfn receptor (TfnR; Trowbridge et al., 1993). The recycling endosome in epithelial cells is increasingly recognized as having roles in trafficking through endocytic, recycling, and exocytic pathways (for reviews see Ellis et al., 2006; van Ijzendoorn, 2006). The recycling endosome in macrophages also subserves both endocytic and exocytic processes, resulting in the delivery of biosynthetic TNFα to the cell surface at sites of phagocytic cup formation (Murray et al., 2005a), along with the recycling endosome membrane required for extension and expansion of the phagocytic cup around captured microbes (Bajno et al., 2000; Cox et al., 2000; Murray et al., 2005a). Although this represents a particularly efficient pathway for the release of TNFα, whether other cytokines are secreted via recycling endosomes and, indeed, via phagocytic cups is not known.

To address this, we directly compared the trafficking and secretion of endogenous and fluorescently tagged TNFα and IL-6 in activated macrophages. We show that IL-6 is loaded into tubulovesicular structures that bud off the TGN and fuse with recycling endosomes in transit to the plasma membrane. Surprisingly, in macrophages simultaneously producing TNFα and IL-6, it became clear that the trafficking of these two cytokines use overlapping but distinct trafficking pathways. Importantly, both TNFα and IL-6 are delivered to recycling endosomes but still maintain the ability to exit independently from this endosomal compartment.

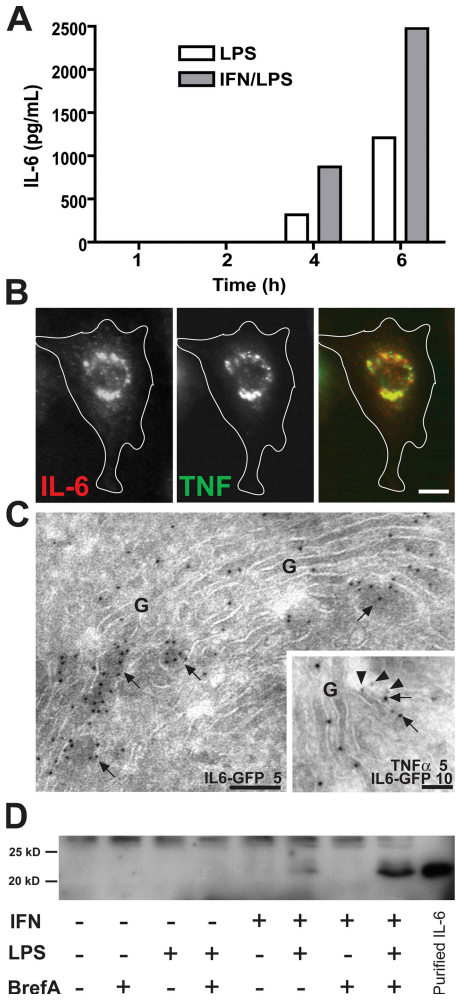

Figure 1. **Expression of IL-6 and TNFα in macrophages.** (A) RAW264.7 cells were stimulated with 100 ng/ml LPS and 500 pg/ml IFNγ, and samples of the medium were removed every 2 h over a 6-h time course. The graph shows the levels of IL-6 as determined by cytokine-specific ELISA secreted by macrophages over the time course. (B) Macrophages were activated with LPS and IFN for 6 h before fixation, permeabilization, and staining for intracellular IL-6 (red) and TNFα (green). Epifluorescence staining shows the coexpression of endogenous IL-6 and TNFα and their coaccumulation in the perinuclear Golgi complex. (C) Immuno-EM of newly synthesized cytokines in Golgi complexes (G), demonstrating IL-6–GFP (arrows) alone or together with TNFα (arrowheads), labeled with 5 or 10 nm gold particles as indicated. (D) Cells were activated with combinations of LPS and IFN for 6 h in the presence or absence of 5 μg/ml brefeldin A, and IL-6 in cell extracts was determined by Western blotting. Consistent with the ELISA data, increased levels of intracellular IL-6 are stimulated in the presence of IFN and LPS together, and disruption of the Golgi complex leads to the intracellular accumulation of IL-6. Bars (B), 5 μm; (C) 100 nm.

Results

Temporal secretion of IL-6 and TNFα in activated macrophages

We have previously described the rapid production and secretion of TNFα from LPS-stimulated RAW264.7 macrophages (Shurety et al., 2000). Accumulation of TNFα precursors can be seen in the Golgi complex by 20 min, and secretion of TNFα can be detected as early as 40 min after LPS stimulation. A high level of secretion is maintained for 4–6 h before declining (Shurety et al., 2000). In response to LPS, low levels of the soluble cytokine IL-6 can also be detected in the supernatant of activated macrophages from 4 h (Fig. 1 A); however, its accumulation in the Golgi complex is not visible until 6 h after stimulation. Priming and activation of macrophages with IFNγ and LPS led to substantially higher levels of IL-6 secretion (Fig. 1 A) and high levels of intracellular IL-6 by 6 h after stimulation. Thus, there is a considerable temporal overlap in the secretion of these two proinflammatory cytokines from activated macrophages. Consistent with this, dual-color immunofluorescence microscopy revealed the simultaneous localization of both IL-6 and TNFα in the Golgi complex in macrophages

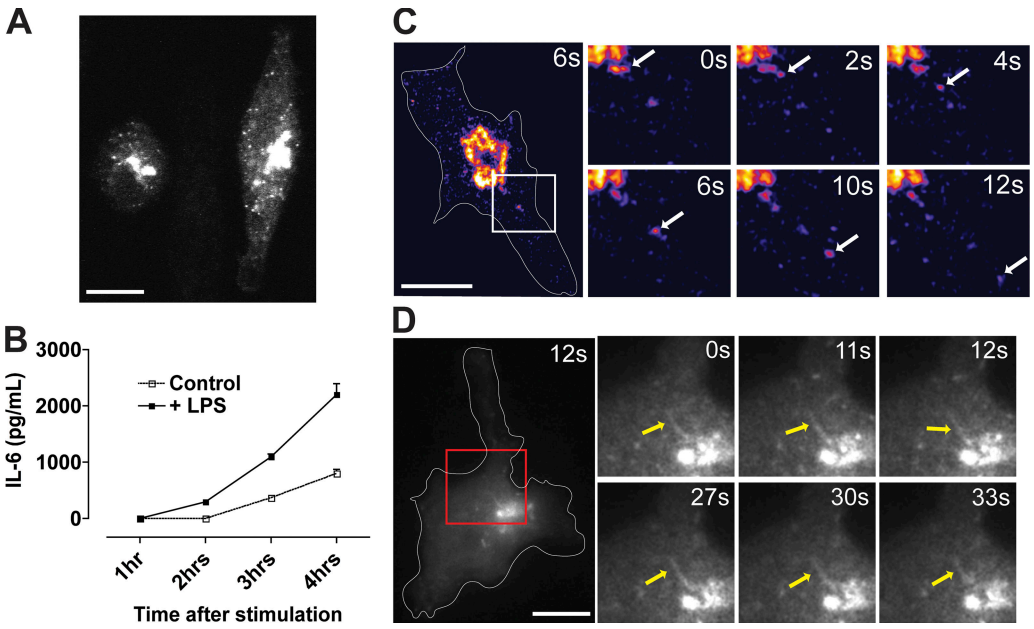

Figure 2. **Trafficking of fluorescently tagged IL-6.** Macrophages were transfected with IL-6–GFP and activated with LPS and IFN for 4 h. (A) Epifluorescence image shows the localization of IL-6–GFP to the Golgi complex and in vesicular structures. (B) Secretion of IL-6 from transfected macrophages in the absence (control) and presence (+LPS) of LPS stimulation as measured by cytokine-specific ELISA. Error bars represent SEM of triplicate transfections in a single experiment. (C and D) Live imaging of transfected macrophages showing IL-6–GFP exiting the Golgi complex in both vesicular (C) and tubular (D) structures. In C, an intensity-based color display pallet was used to emphasize vesicular structures. In the enlarged images (magnified images of boxed areas), arrows are used to highlight single trafficking events or tubules. Bars, 10 μm.

stimulated with IFN and LPS for 6 h (Fig. 1 B). This localization of IL-6 and TNFα to the Golgi stacks was also confirmed by immuno-EM (Fig. 1 C).

A signal sequence in the translated IL-6 protein drives its delivery into the endoplasmic reticulum, but, to confirm its passage through the Golgi complex and the constitutive secretory pathway, macrophages were stimulated in the presence of brefeldin A, a drug known to disrupt the structure and secretory function of the Golgi complex. This treatment led to the substantial accumulation of intracellular IL-6 within activated macrophages (Fig. 1 D) and completely blocked IL-6 secretion into the medium (not depicted).

IL-6 exits the TGN in tubulovesicular carriers

In fixed cells, endogenous IL-6 can be immunostained and clearly observed in the Golgi region (Fig. 1 B), but no other organelles or cytoplasmic vesicles containing this soluble cytokine were readily visible, probably because of the insufficient density of the cytokine during trafficking. Therefore, to track the secretory pathway of IL-6, we generated fluorescently tagged constructs containing the full-length sequence of IL-6 (GFP–IL-6 and mCherry–IL-6) and induced the expression of these constructs by transient transfection of macrophages. Within 4 h after transfection, high levels of fluorescently tagged IL-6 are visible within the Golgi complex (Fig. 2 A), where immuno-EM shows the soluble cargo accumulating in the dilated ends of Golgi cisternae (Fig. 1 C). IL-6–GFP was now also present in large vesicular structures throughout the cytoplasm. The fluorescently tagged IL-6 is actively secreted from macrophages even in the absence of exogenous stimulation, but higher levels are secreted from LPS-stimulated cells (Fig. 2 B). All IL-6 detected in this ELISA is presumably GFP tagged, as no endogenous IL-6 is secreted from mock-transfected cells, and, after LPS stimulation, only very low levels were detected at the 4-h time point (unpublished data). Thus, the expression of fluorescently tagged IL-6 is a suitable model with which to study IL-6 biosynthetic trafficking.

Live imaging of IL-6–GFP-transfected cells was performed to visualize its exit from the TGN and subsequent post-Golgi movement. As highlighted in Fig. 2 C and Video 1 (available at http://www.jcb.org/cgi/content/full/jcb.200612131/DC1), vesicular structures were readily observed leaving the brightly stained Golgi pool of IL-6–GFP. In addition, large tubular structures containing IL-6–GFP were observed in some cells as they exited the Golgi region. These structures were often maintained for >30 s, and vesicular structures budding off the Golgi complex were also observed in these same cells (Fig. 2 D and Video 2). These carriers are similar in form and kinetics to those described previously for TNFα transport (Murray et al., 2005a), leading us to compare the trafficking of these cargoes.

IL-6 is loaded into post-Golgi carriers with and without TNFα

Live imaging of cells coexpressing TNFα-mCherry and IL-6–GFP was performed. Both TNFα-mCherry and IL-6–GFP were visualized exiting the TGN in tubular and vesicular carriers. However, the budding of carriers containing IL-6–GFP was more frequent than for those with TNFα-mCherry, and, most of the time, IL-6–GFP appeared as the sole cargo in budding

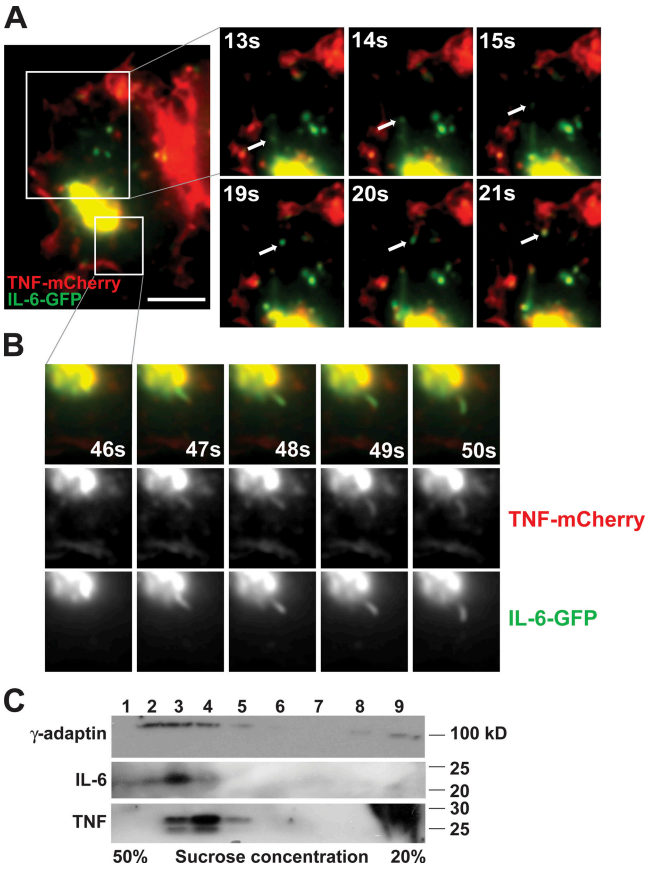

Figure 3. **IL-6 exits the TGN in carriers both with and without TNFα.** (A and B) Live epifluorescence dual-color imaging of macrophages transfected with TNFα-mCherry (red) and IL-6–GFP (green) demonstrating IL-6 leaving the TGN in a carrier devoid of TNFα (A) and in a tubule also containing TNFα (B). Cells were stimulated with LPS and IFNγ before imaging. In the enlarged images, arrows are used to highlight single trafficking events, and the time at which each still frame was collected is labeled. (C) Cell lysates of activated macrophages were fractionated to separate Golgi membranes and cytosol. Golgi membranes were then incubated with the cytosol in an in vitro Golgi budding reaction as described in Materials and methods. Samples from the budded vesicle fractions (labeled 1–9) were resolved and analyzed by Western blotting to detect γ-adaptin as a vesicle-associated protein and IL-6 and TNF as cargoes. Bar, 10 μm.

carriers (Fig. 3 A). In contrast, carriers containing TNFα that budded off the TGN almost always contained IL-6 (Fig. 3 B). A single video depicting both of these trafficking events is provided as Video 3 (available at http://www.jcb.org/cgi/content/full/jcb.200612131/DC1).

A biochemical approach was also used to investigate the localization of TNFα and IL-6 in post-Golgi carriers. Golgi membranes were isolated from homogenates of macrophages stimulated with IFN/LPS for 4 h. Both pro-TNFα and IL-6 were readily detected in these Golgi fractions, which were then incubated in the presence of cytosol and GTPγs to induce budding of Golgi-derived membrane carriers. The resulting budded vesicles were then segregated into different populations by passage over a sucrose density gradient (Heimann et al., 1999; Wylie et al., 1999), and eluted fractions were assayed by Western blotting. IL-6 and TNFα were both present in subsets of the Golgi-derived vesicles that overlapped with the distribution of another vesicle-associated protein, γ-adaptin. IL-6 and TNFα appeared in an overlapping distribution but notably peaked in different vesicle fractions, with IL-6 vesicle carriers in heavier fractions than TNFα-containing carriers (Fig. 3 C). This result is consistent with the live imaging in showing that these two cytokines exit the Golgi complex in carriers that contain cytokines as individual or mixed cargo.

Peripheral structures containing both TNFα and IL-6 correspond to recycling endosomes

In live cells, vesicles budding off the TGN containing IL-6–GFP were observed fusing with large, preexisting stable compartments within the cytoplasm (Fig. 4 A and Video 4, available at http://www.jcb.org/cgi/content/full/jcb.200612131/DC1). In fixed macrophages, IL-6–GFP was also visible in these large peripheral structures, where, in many cases, it colocalized with either TNFα-mCherry or endogenous TNFα (Fig. 4 B). Quantification of these structures containing IL-6–GFP demonstrated that ∼70% colocalize with endogenous TNFα or with TNFα-mCherry (Fig. 4 B), identifying this as a common destination for both newly synthesized cytokines. In light of our previous work demonstrating that TNFα is delivered from the TGN to recycling endosomes (Murray et al., 2005a), we hypothesized that these large structures containing both TNFα and IL-6, as shown in Fig. 4 B, may represent recycling endosomes. Immuno-EM also confirmed the colocalization of TNFα and IL-6 to endosomes and large vesicular structures (Fig. 4 C). Among these structures were some containing IL-6 and TNFα together and others with only one cytokine. Of interest, IL-6 appears to consistently localize to the luminal face of the membrane, which is suggestive of membrane association.

To formally investigate the recycling endosome as a site for TNFα and IL-6 delivery, high resolution confocal microscopy was performed on cotransfected fixed cells. We have previously shown that vesicle-associated membrane protein 3 (VAMP3) is a reliable marker of recycling endosomes in macrophages (Murray et al., 2005a), with its expression leading to the localization of this SNARE protein to ringlike structures that represent recycling endosomes. Coexpressed IL-6–mCherry strongly localized to these VAMP3-positive ringlike recycling endosomes, as highlighted by the inset in Fig. 5 A. In other cases, the known recycling endosome cargo of internalized Tfn was used in conjunction with the overexpression of IL-6–GFP and TNFα-mCherry. Fig. 5 B clearly shows several structures that contain both GFP-TNFα and IL-6–mCherry (indicated by arrows) and also colocalize with internalized Tfn, which is consistent with their identity as recycling endosomes. The localization of IL-6 and TNFα in recycling endosomes was also confirmed by immuno-EM, in which the cytokines colocalized with TfnR (Fig. 5 C) in both peri-Golgi and more peripheral recycling endosomes. Quantification showed that 51% of labeled structures contained IL-6 alone, whereas 29% of TfnR-labeled endosomes were also co-labeled for IL-6; this included structures in which the TfnR and IL-6 gold particles were at opposite ends of tubules. Similarly, 72% of labeled endosomes had TNFα alone, whereas 14% were co-labeled with TfnR. Thus, a substantial proportion of recycling endosomes, or parts thereof, contain each cytokine as a single cargo.

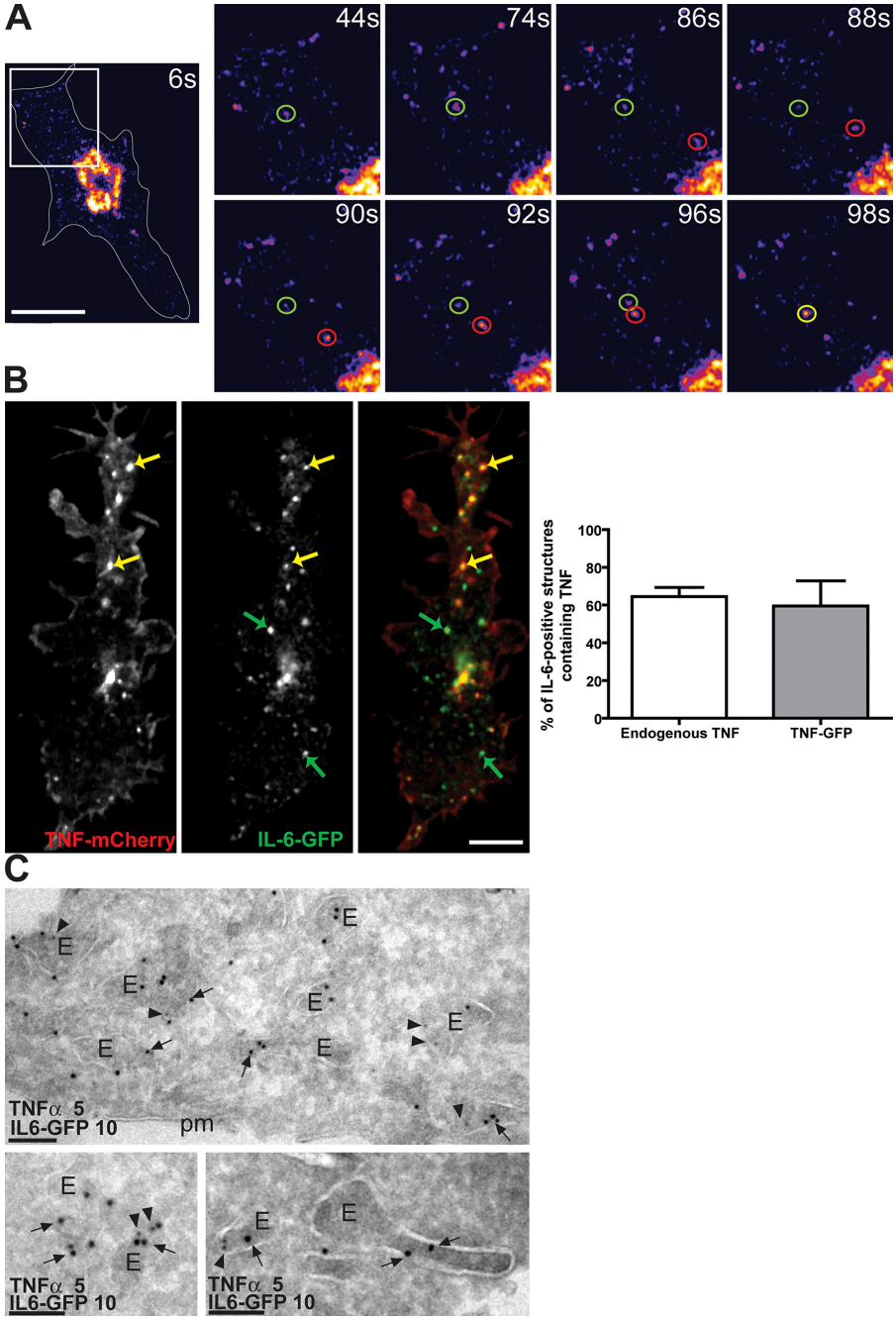

Figure 4. **A large proportion of vesicular IL-6 colocalizes with TNFα.** (A) Live epifluorescence microscopy of an IL-6–GFP-transfected macrophage showing fusion of a post-TGN carrier (red circles) with a large preexisting IL-6–containing structure (green circles), possibly a recycling endosome. A yellow circle highlights the resulting fused structure. An intensity-based color display pallet was used to emphasize vesicular structures, and the time each was captured is indicated. (B) High resolution confocal microscopy on macrophages cotransfected with IL-6–GFP (green) and TNFα-mCherry (red) revealed overlap in the localization of IL-6 and TNFα in structures toward the cell periphery (yellow arrows). Green arrows highlight structures that contain IL-6 alone. Quantification of colocalization revealed that in macrophages, ~60–70% of the IL-6–positive structures also contain either endogenous TNFα or overexpressed TNFα. More than 20 IL-6–GFP-expressing cells were measured to generate each set of data, and error bars represent means ± SEM. (C) Immuno-EM of IL-6–GFP (arrows) and TNFα (arrowheads) labeled with 10 nm or 5 nm gold particles, respectively, in peripheral endosomes (E), some of which are in the vicinity of the plasma membrane (pm). Individual endosomes have IL-6–GFP alone or together with TNFα. Bars (A), 10 μm; (B) 5 μm; (C) 100 nm.

Based on a fluorescence intensity line scan through several recycling endosomes (Fig. 6 A), we noted that Tfn did not always peak precisely with TNFα and IL-6, but, instead, all three proteins appeared in very close proximity. In the structures containing IL-6, the peak fluorescence overlaps tightly with the peak of TNFα (Fig. 6 A, structures 2 and 3), but Tfn fluorescence is more dispersed in these structures compared with those containing TNFα and Tfn alone (Fig. 6 A, structures 1 and 4). This raises two questions: are all three of these cargoes truly localizing to the same structure, and, if so, are they segregated within that structure?

To address these questions, two different approaches were undertaken. First, 3D reconstructions of recycling endosomes containing IL-6, TNFα, and Tfn were performed to access the distribution of cargo within these structures. Specified recycling endosomes were excised and subjected to surface rendering, allowing their visualization in 3D (Fig. 6 B). In structure A, IL-6 overlaps with TNFα, and Tfn appears to occupy a separate domain within this structure. In contrast, structure B contains substantial amounts of all three cargoes, but each occupies a separate domain, with very little direct overlap. These images clearly suggest the existence of the dynamic compartmentalization of cargoes within the recycling endosome. A second approach was used to confirm that cargoes are in a single recycling endosome. Cells expressing IL-6–GFP were sequentially incubated in the presence of the $DiIC18_{(5)}$-DS lipophilic dye followed by a chase

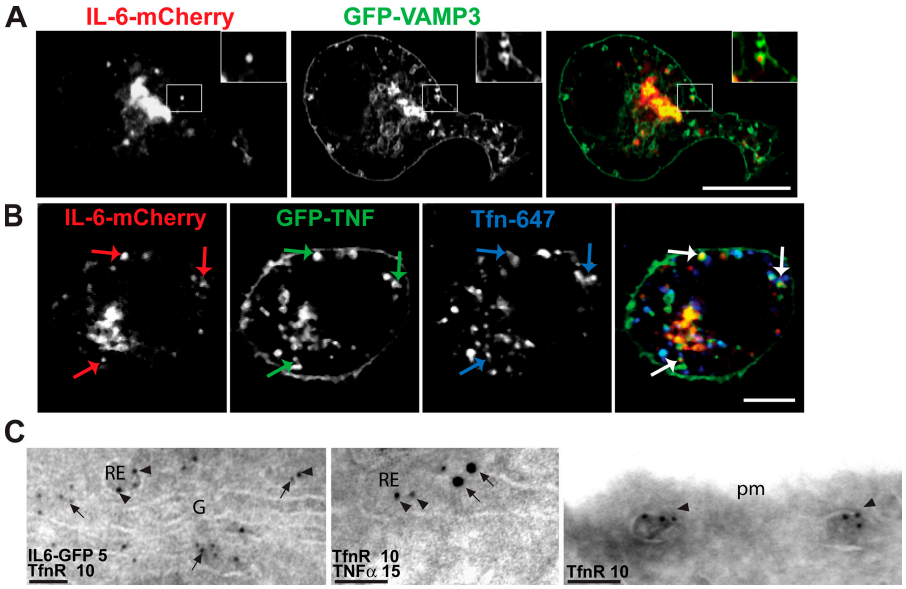

Figure 5. **IL-6 and TNFα colocalize in the recycling endosome.** (A and B) RAW264.7 cells were transfected with IL-6–mCherry and either GFP-VAMP3 (A) or GFP-TNFα (B) and activated with LPS and IFN for 4 h before fixation. In addition, to label transfected cells with Tfn (blue), macrophages were incubated in the presence of AlexaFluor647-conjugated Tfn (B). Cells were imaged via high resolution confocal microscopy. (A) A large proportion of IL-6–positive structures colocalize with the recycling endosome markers VAMP3 (A), endocytosed Tfn, and TNFα (B). In A, the insets highlight single ring-shaped VAMP3-positive structures containing IL-6. In B, colored arrows are used to highlight three recycling endosome structures containing all three cargo proteins. (C) Immuno-EM of IL-6–GFP, endogenous TfnR, and TNFα labeled with 5, 10, or 15 nm gold particles. Peri-Golgi (left) or peripheral (middle and right) recycling endosomes (RE) are labeled with TfnR, which is recycling from the plasma membrane (pm; right). IL-6–GFP or TNFα (arrows) colocalized with TfnR (arrowheads) in recycling endosomes. G, Golgi complex. Bars (A), 10 μm; (B) 5 μm; (C) 100 nm.

period devoid of dye in which the cells were incubated with Texas red–conjugated Tfn. The lipophilic dye initially labels the plasma membrane, but, under this protocol, it is internalized into all surface-derived endosomes. In Fig. 6 C, a structure is highlighted where IL-6 and Tfn are found side by side but are linked within the same endosomal structure by the overlap of both cargoes with lipophilic dye. Thus, dye labeling helps to demonstrate that IL-6 and Tfn can exist in the same recycling endosome but occupy separate regions of the compartment. Collectively, our results show that IL-6 and TNFα are delivered to the same recycling endosome but can be segregated as cargo within the recycling endosome, with each also being able to be segregated from the internalized cargo Tfn. Thus, the recycling endosome has the potential to compartmentalize cargo.

SNARE-mediated trafficking of IL-6 via the recycling endosome

We have previously described a Q-SNARE complex consisting of Vti1b, syntaxin 7 (Stx7), and Stx6 on post-Golgi carriers that mediates the trafficking of TNFα from the TGN to the recycling endosome in activated macrophages (Murray et al., 2005a,b). In the present study, we sought to examine whether some of these SNARE proteins also function in IL-6 trafficking. Transient overexpression of the TGN-localized Q-SNARE proteins Stx6 and Vti1b led to significant increases ($P < 0.05$) in the level of IL-6 secretion compared with controls or with cells transfected with an irrelevant SNARE, Stx2, or an unrelated TGN protein, mannose-6-phosphate receptor (M6PR; Fig. 7 A). In addition, siRNA knockdown of Stx6 and particularly of Vti1b significantly decreased ($P < 0.05$) the level of IL-6 secretion in cultures in which 50–70% of cells demonstrated knockdown of the relevant gene (Fig. 7 B). Thus, it is likely that the same Q-SNARE complex, perhaps in addition to others, regulates the post-Golgi traffic of IL-6. VAMP3 on the recycling endosome is the complementary R-SNARE for this transport step, and its overexpression or siRNA knockdown both affect TNFα trafficking (Murray et al., 2005a). Transient overexpression of VAMP3 here resulted in a significantly increased ($P < 0.05$) secretion of IL-6 (Fig. 7 C). Similarly, siRNA knockdown of VAMP3 decreased IL-6 secretion (Fig. 7 D). This is functional evidence that endogenous IL-6 is trafficked via the recycling endosome for secretion and that these SNAREs can regulate both TNFα and IL-6 trafficking.

To test whether the recycling endosome is an essential intermediary for IL-6 secretion, an endosomal inactivation assay was performed as previously described (Futter et al., 1995; Ang et al., 2004; Murray et al., 2005a). Inactivation of recycling endosome function by sequestration and activation of HRP-Tfn blocks the secretion of TNFα, (Murray et al., 2005a), and, in this study, we show that IL-6 secretion is similarly and completely blocked under these same conditions (Fig. 7 E). This block occurs at a post-Golgi step at recycling endosomes because Golgi staining of IL-6 and TNFα is still visible in endosome-inactivated cells. Quantification shows a big increase in cells showing Golgi-accumulated TNFα and a small decrease in cells with Golgi-accumulated IL-6, perhaps revealing a difference in the accumulation of membrane-bound and soluble cargo under conditions in which subsequent trafficking and secretion are blocked (Fig. 7 F). Alternatively, this decrease in the number of cells producing IL-6 may result from the blockage of TNF secretion, which is known to have an autocrine effect on macrophages and enhance subsequent cytokine secretion. These results confirm that the recycling endosome has a pivotal functional role as an intermediate compartment during the secretion of cytokines from activated macrophages.

Differential trafficking of IL-6 and TNFα during phagocytic cup formation

We have recently shown that TNFα in the recycling endosome is trafficked to the phagocytic cup along with membranes

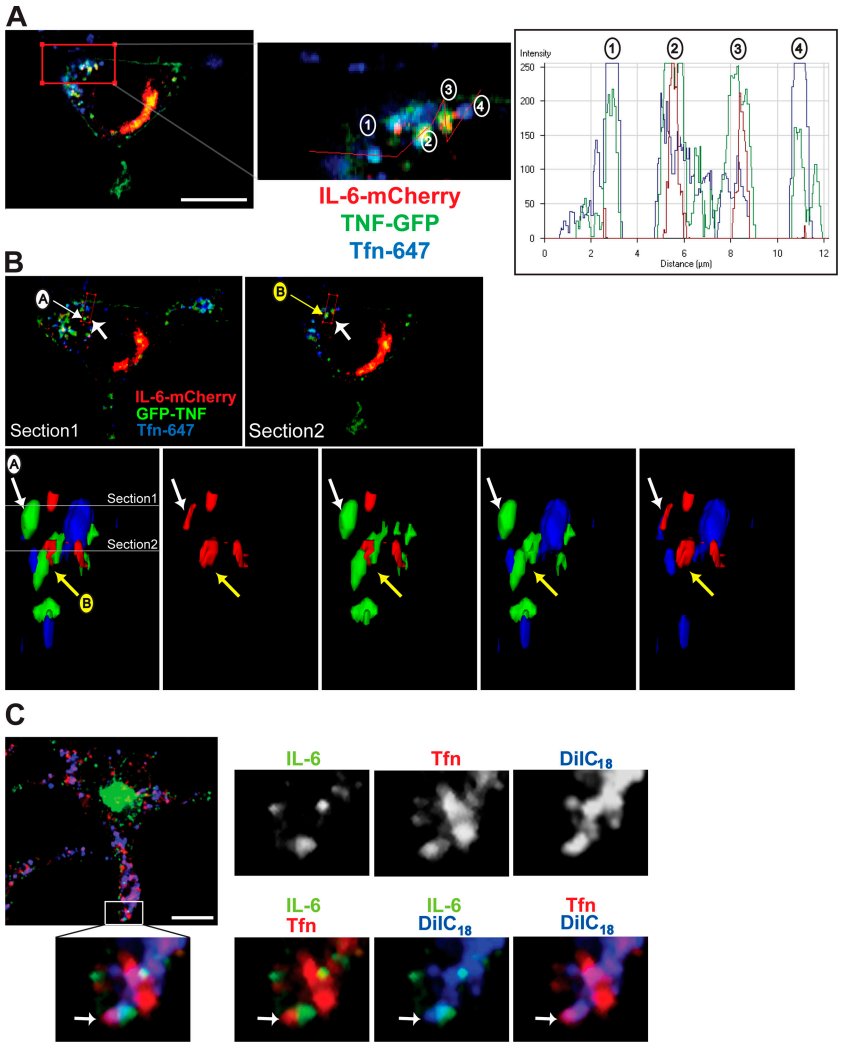

Figure 6. **Compartmentalization of endosomal structures containing IL-6, TNFα, and Tfn.** (A–C) Macrophages were transfected with fluorescently tagged IL-6 (C) or both IL-6–mCherry and TNF-GFP (A and B) and were subsequently incubated in the presence of fluorescently conjugated Tfn. In A, a fluorescence intensity line scan profile was generated along the red line, with fluorescence peaks for the four recycling endosomes highlighted. In IL-6–positive structures, the peak fluorescence appears to overlap with the peak of TNFα (structures 2 and 3), but the Tfn fluorescence is more dispersed in these structures compared with those containing TNFα and Tfn alone (structures 1 and 4). (B) Two confocal sections are shown highlighting recycling endosome structures, which are labeled A and B. The enlarged area represents a surface-rendered 3D image of the region highlighted. Images are viewed in the direction of the large arrows and in the cross section through the cell. This demonstrates examples of recycling endosomes with both overlapping and discrete domains for each of the markers. In C, transfected macrophages were additionally subjected to labeling using the $DiIC_{18}(5)$-DS lipophilic dye (blue) before incubation with Tfn (red) as described in Materials and methods. The enlarged area shows Tfn and IL-6 labeling separate domains within a single dye-positive endosomal structure (highlighted by white arrows). Bars (A), 5 μm; (B and C) 10 μm.

recruited during phagocytosis (Murray et al., 2005a). Therefore, a central question becomes whether IL-6 is also delivered to the cell surface via the phagocytic cups. As soluble cargo, IL-6 is released immediately from cells, and it is not normally stained at the cell surface. Therefore, the movement of IL-6–GFP in the vicinity of phagocytic cups was examined in live cells. When videos of cells coexpressing VAMP3-GFP and mCherry–IL-6 were analyzed by particle tracking software, compilations of the tracks taken by these two proteins over time reveal different targeting (Fig. 8 A). Although VAMP3-GFP tracks show concerted movement toward and directly around a phagocytic cup, there are no mCherry–IL-6 tracks leading toward or even in the vicinity of the phagocytic cup in this and other examples. In no experiments using live or fixed cells did we detect IL-6 around or near phagocytic cups, suggesting that it and TNFα are segregated and are targeted distinctly upon exit from the recycling endosome. TNFα is delivered to the phagocytic cups, but IL-6 is not.

The selective targeting of recycling endosome cargo to the phagocytic cup was also examined in the case of TfnR. Macrophages phagocytosing yeast could be seen with VAMP3-GFP and TNF-GFP at the actin-rich phagocytic cups, but, in contrast, TfnR was not concentrated at the cups (Fig. 8 B). This confirms that there is selective delivery of cargo such as TNFα to the phagocytic cup, but other cargo, such as IL-6 and TfnR, are excluded from movement to this site. This is a functional demonstration of cargo within the recycling endosomes being compartmentalized.

We also demonstrate that different cargo can exit the recycling endosome separately. In live cells coexpressing IL-6–GFP and TNF-mCherry, we see both cytokines together in recycling endosomes, and Fig. 9 A (also see Video 5, available at http://www.jcb.org/cgi/content/full/jcb.200612131/DC1) shows the exit of IL-6–GFP from this structure in a carrier but not of TNF-mCherry. In addition, in a macrophage undergoing phagocytosis of an IgG-coated bead, VAMP3 can be seen exiting a recycling endosome independently of IL-6, which is retained while VAMP3 moves in a carrier toward a phagocytic cup (Fig. 9 B and Video 6). Thus, cargo delivered to the recycling endosomes is compartmentalized, presumably undergoing sorting, and can then exit in specific carriers that are targeted to different destinations. The recycling endosome in the macrophage has final and selective control over the fate and destination of its proinflammatory cytokines.

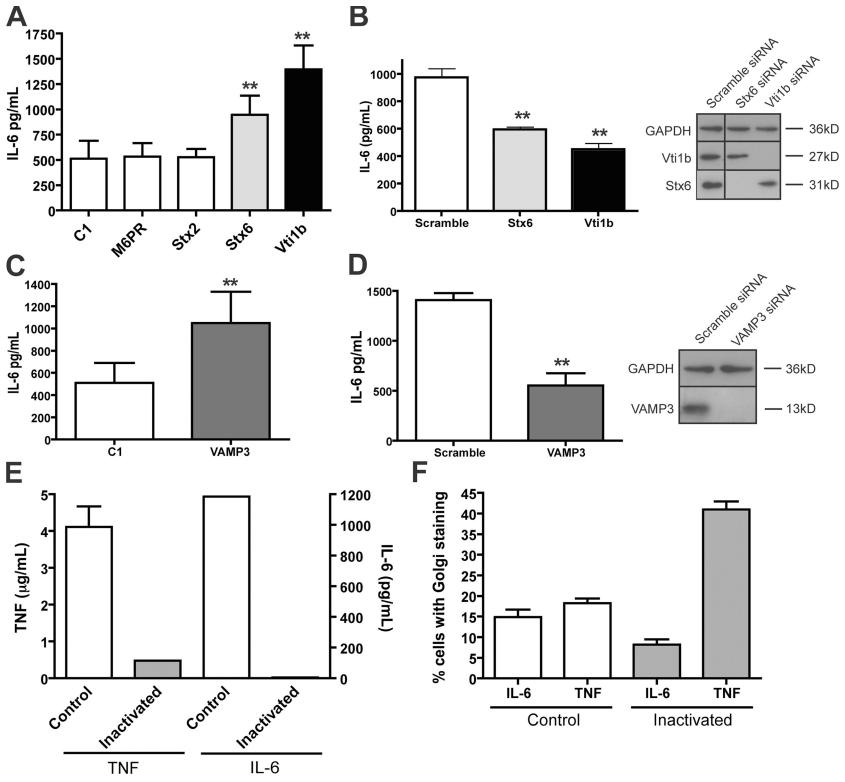

Figure 7. **SNARE and recycling endosomes in the trafficking and secretion of IL-6.** (A–F) Exocytic trafficking was altered in macrophages by the overexpression of specific SNAREs (A and C), their knockdown by specific siRNA (B and D), or by HRP inactivation of the endocytic compartment (E and F). After transfection or treatments, the macrophages were activated with LPS and IFN, the medium was collected 2 h and 6 h after stimulation, and the levels of IL-6 and/or TNFα, respectively, were determined by cytokine-specific ELISAs. (A and C) Overexpression of Stx6, Vti1b, and VAMP3 but not Stx2 led to increased levels of IL-6 secretion from macrophages. Bar graphs represent means ± SEM (error bars) of triplicate transfections. (B and D) Targeted knockdown of the Q-SNAREs Vti1b, Stx6, and VAMP3 by siRNA resulted in significant decreases in the level of IL-6 secreted from activated macrophages. Lysates of macrophages subjected to siRNA knockdown were blotted for Vti1b, Stx6, VAMP3, and the loading control protein glyceraldehyde-3-phoshphate dehydrogenase (GAPDH). Bar graphs represent mean ± SEM of triplicate siRNA transfections. (E) HRP inactivation of the endosomal compartment as described in Materials and methods blocked the secretion of both TNFα and IL-6. (F) In addition, after 6 h of stimulation, coverslips were fixed, stained for intracellular TNFα and IL-6, and the percentage of cells expressing each cytokine was determined. 10 low magnification images were captured per assay condition, each containing at least 50 cells, and the percentage of cells producing TNFα and/or IL-6 was calculated (D). Bar graphs represent mean percentages ± SEM of the individual images captured. **, $P < 0.05$.

Discussion

By examining endogenous IL-6 and fluorescently tagged IL-6 in live and fixed macrophages, we describe here, for the first time, the secretory pathway for the soluble cytokine IL-6. Fluorescent IL-6 was observed exiting the Golgi complex in tubulovesicular carriers, where it appeared as labeled cargo alone or in conjunction with TNFα. Overall, our results are in agreement with the limited observations of intracellular IL-6 in the literature, including an early study showing the costaining of TNFα and IL-6 in the Golgi complex of activated monocytes (Andersson and Matsuda, 1989) and electron microscopic labeling showing that, as a constitutive secretory product in mast cells, IL-6 was excluded from entry into secretory granules and was instead found clustered in small constitutive vesicles after leaving the Golgi complex (Kandere-Grzybowska et al., 2003). Now, a major revelation in this study is that IL-6, upon leaving the Golgi complex, is trafficked to the recycling endosome before it is delivered to the cell surface. Moreover, we show that the recycling endosome represents a critical point of divergence for the cytokines IL-6 and TNFα, with TNFα but not IL-6 delivered to phagocytic cups. Compartmentalization of cargo within the recycling endosome underpins the individual exit and release of these cytokines, revealing new capacities and an important role for this organelle in orchestrating the macrophage immune response.

Fluorescent IL-6 is loaded into tubulovesicular structures budding from the TGN in live macrophages. The size, appearance, and kinetics of these carriers are consistent with carriers seen previously in macrophages labeled with TNFα as cargo, and they are also similar to post-Golgi carriers visualized in other cell types (Polishchuk et al., 2000, 2006; Lock et al., 2005; Murray et al., 2005a). By immunofluorescence, EM, and biochemical analyses, we show that IL-6 is the lone labeled cargo in some carriers, whereas in other cases, it is in carriers that also contain TNFα. Although TGN-derived carriers containing fluorescent IL-6 were abundant (for example, see Video 3), those containing TNFα alone or IL-6 were seen less frequently. Thus, there is little apparent sorting of soluble cargo like IL-6 at the TGN, whereas membrane-bound TNFα must be actively sorted for more selective loading into carriers. This is also borne out by previous data from HeLa cells, in which we showed that TNFα is selectively loaded into only a subset of golgin-labeled carriers budding off the TGN (Lock et al., 2005). In general, there is little understanding of how soluble cargo in constitutive secretory pathways is handled at the TGN. Other soluble cargo such as the lysosomal enzyme is sorted in the TGN by binding to M6PR for trafficking to endosomes (Ghosh et al., 2003), and, in cells with regulated secretion, secretory products are clustered by binding to chromogranins in the TGN for loading into secretory granules (Kim et al., 2001; Arvan et al., 2002). An earlier study suggests that in epithelial cells, soluble proteins are sorted in a pH-dependent compartment for polarized delivery to the cell surface (Caplan et al., 1987). Our current findings now highlight the fact that the TGN may not be the only place for the sorting of biosynthetic cargo such as cytokines. The recycling endosome, which is appropriately slightly acidic (Teter et al., 1998; Gagescu et al., 2000), must now also be considered as a possible sorting site for membrane-bound (Rodriguez-Boulan and Musch, 2005) and soluble cargoes.

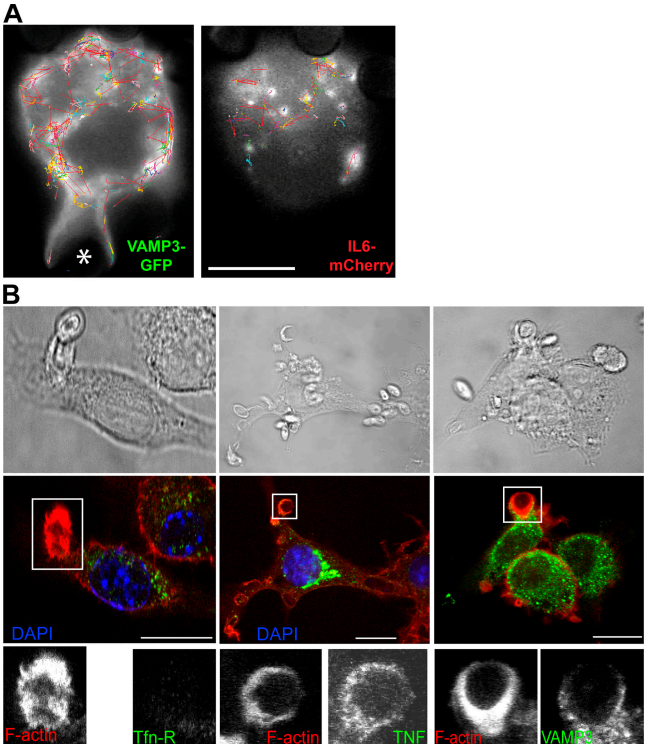

Figure 8. **Delivery of TNFα and VAMP3 but not IL-6 or TfnR from recycling endosomes to the phagocytic cup.** (A) Dual-color live imaging of the phagocytosis of IgG-opsonized 3-μm latex beads by macrophages transfected with VAMP3-GFP (green) and IL-6–mCherry (red). An overview of all particle tracks over a 10-min time course (200 frames) is shown. The tracks were filtered so only those that were continuous for five or more frames are displayed. Each detected track is shown at its full length as a continuous color, with red sections being interpolated by the software to handle occlusion, exit, and entry of a particle along the trajectory. VAMP3 can be seen to have extensive movement around and toward the forming phagocytic cup, which is in contrast to IL-6, which never advances to the cup. The location of the particle being phagocytosed is indicated with an asterisk. (B) IFN-primed macrophages were incubated for 10 min with *C. albicans* and were fixed and stained with DAPI (blue; nucleus) and for F-actin (red; highlighting sites of phagocytic cup formation), VAMP3, TNFα, and transferrin receptor (TfnR). Top panels show phase-contrast images to highlight the location of the yeast. Boxed areas are enlarged to show staining at the actin-rich phagocytic cups. Bars (A), 5 μm; (B) 10 μm.

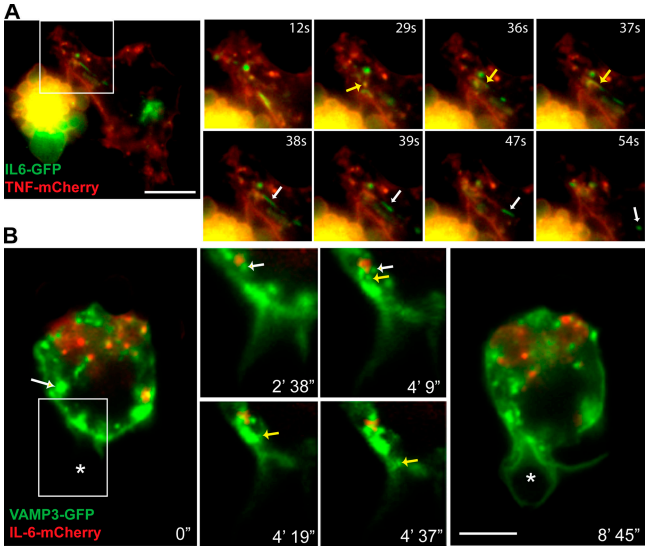

Figure 9. **Trafficking of IL-6 from recycling endosomes can be regulated independently of other recycling endosome functions.** (A) Dual-color live imaging of macrophages transfected with IL-6–GFP (green) and TNFα-mCherry (red). Enlarged images demonstrate the tubulation of a structure containing both TNFα and IL-6 (yellow arrows), with IL-6 alone budding off (white arrows) to form a new vesicle. (B) Dual-color live imaging of the phagocytosis of IgG-opsonized 3-μm latex beads by macrophages transfected with VAMP3-GFP (green) and IL-6–mCherry (red). Frames from the dual-color video were extracted to highlight the movement of vesicles containing VAMP3 (yellow arrow) but not IL-6, budding off a recycling endosome containing both cargoes (white arrows), and trafficking toward the phagocytic cup. The phagocytosing bead is highlighted with asterisks. Boxed areas are magnified at the right. Bars (A), 10 μm; (B) 5 μm.

Several lines of evidence show that the post-Golgi carriers containing IL-6 are indeed delivered to recycling endosomes. First, overexpression or knockdown of the SNARE proteins Vti1b, Stx6, and VAMP3 affected the secretion of IL-6. We have previously shown that these proteins are part of the Q-SNARE complex (Stx6–Stx7–Vti1b) on the TGN with the cognate R-SNARE VAMP3 on recycling endosome membranes and that this complex regulates TNFα trafficking in macrophages (Murray et al., 2005b). Implicating these SNAREs also in IL-6 trafficking is consistent with both cytokines sharing some carriers and/or being trafficked in separate carriers regulated by the same SNAREs, although it is possible that additional SNARE complexes could be involved. VAMP3 function in IL-6 secretion confirms the recycling endosome as a post-Golgi destination for this cytokine. Second, by live cell imaging, fluorescently tagged IL-6 in tubular and vesicular carriers budding off the TGN was frequently observed fusing with preexisting recycling endosomes in the cell periphery. In these same structures, IL-6 was colocalized with recycling endosome markers, including VAMP3 and endocytosed Tfn. Finally, inactivation of the recycling endosome completely ablated the secretion of IL-6, showing that this is a requisite compartment en route to the cell surface for newly synthesized IL-6. The direct delivery of all or most of IL-6 to the recycling endosome is in agreement with the transport of other biosynthetic cargo from the TGN to this compartment, including TNFα in macrophages and endothelial cadherin and vesicular stomatitis virus-G in epithelial cells (Ang et al., 2004; Lock et al., 2005). IL-6 is the first example of a constitutively transported soluble cargo trafficking to the cell surface via the recycling endosome, and, as such, it underscores the diverse roles played by the recycling endosome in exocytosis.

The recycling endosome handles cargo from both endocytic/recycling routes as well as exocytic cargo (for review see van Ijzendoorn, 2006). In the present study, we present evidence that IL-6 and TNFα converge with recycling Tfn and with the resident SNARE VAMP3 within recycling endosomes. Importantly, however, all three of these cargo proteins appear to be partially segregated within this compartment based on colocalization and image reconstruction in fixed and live cells. This compartmentalization differentiates not only recycling and exocytic cargo but even segregates different exocytic cargo within the same structure. Live imaging and image reconstructions demonstrate that such a compartmentalization of cargo is an

extremely dynamic process, with cargo-rich domains that continuously merge and then segregate (Video 3). Mechanisms for sorting and compartmentalizing the membrane-bound cargoes such as TNFα and Tfn/TfnR can be envisioned, but very little is known about how soluble proteins are or could be sequestered (Rodriguez-Boulan et al., 2005; for review see Ellis et al., 2006). It is possible that surface receptors for IL-6, such as IL6R or gp130 (Kishimoto et al., 1995), could be involved, but this awaits further investigation. In addition, it is notable that IL-GFP switched from accumulating in the lumens of Golgi cisternae to being on the luminal face of recycling endosome membranes in our immuno-EM images. This is suggestive of membrane association that could provide a mechanism for IL-6 in sorting at the level of the recycling endosome.

The concept of having compartmentalized recycling endosomes is already soundly established within the literature, particularly with reference to the membrane-associated trafficking machinery. Light, fluorescence, and EM studies show this to be a highly reticulated and tubular compartment (Ullrich et al., 1996; Cox et al., 2000; Ang et al., 2004; Lock et al., 2005). It has a complex and segmented molecular landscape with multiple resident GTPases such as Arf6 and the Rab11 subfamily proteins (Casanova et al., 1999; Schlierf et al., 2000; Powelka et al., 2004). Members of the Rab11 family demark different compartments of the recycling endosome in MDCK cells with the locations of Rab11a and Rab25 distinct from that of Rab11b (Lapierre et al., 2003). Similarly, the large Rab11-FIP family of Rab11a effectors offers many opportunities for further spatial and functional complexity, as does another Rab11 effector, myosinVb, which has also been shown to differentially regulate different cargo trafficking through the recycling endosome (Meyers and Prekeris, 2002; Lapierre and Goldenring, 2005; Jin and Goldenring, 2006). Resident recycling endosome markers such as Rab11 and the SNARE VAMP3 only partially colocalize with Tfn as cargo (Ullrich et al., 1996; Teter et al., 1998). A targeted fluorescence method used by Teter et al. (1998) showed only a 20–30% overlap between Tfn and VAMP3 on pericentriolar recycling endosomes. There is also a dynamic overlap or continuity of recycling endosomes with early endosomes, as demonstrated by the sequential but overlapping distributions of Rabs 11, 4, and 5, portending the possibility of recycling endosomes being part of a continuous tubular network (Daro et al., 1996; Ullrich et al., 1996; Teter et al., 1998; Sonnichsen et al., 2000; Bonifacino and Rojas, 2006). Thus, the complex handling and segregation of cargoes within the recycling endosome that we show here now suggests a functional consequence for this array of machinery found associated with these membranes.

TNFα and IL-6 are both proinflammatory cytokines that are secreted temporally in overlapping profiles from macrophages, but, because both cytokines have different immune functions, it is important for their secretion to be tightly coordinated throughout the inflammatory response. In this study, we show for the first time that the secretion of these cytokines can be differentially regulated at the level of intracellular trafficking in addition to their known regulation at the transcriptional and translational levels (Kracht and Saklatvala, 2002). Similarly, Huse et al. (2006) recently identified the existence of two separate exocytic pathways for the targeted or polarized trafficking of cytokines to the immunological synapse or to the entire plasma membrane in activated T cells. This bears analogy to the targeted delivery of TNFα directly to the phagocytic cup and the more generalized secretion of IL-6, which is shown here in macrophages. It is not known whether the recycling endosome is involved in the differential trafficking of cytokines in T cells, as we show here for macrophages. Our results may also be comparable with the differential release of IL-4 and -12 from eosinophil crystalloid granules (Moqbel and Coughlin, 2006; Spencer et al., 2006). In these granules, IL-4 is selectively mobilized to move from the granules into secretory vesicles by IL-4Rα after the stimulation of eosinophils (Spencer et al., 2006). Such examples highlight the importance for immune cells to independently regulate and release cytokines. Indeed, by analogy, we propose that this is a function assigned to recycling endosomes in macrophages, which, unlike granulocytes, do not have granules for packaging and selective release of cytokines.

Unlike TNFα, the secretion of IL-6 was not linked to the formation of phagocytic cups. This possibly reflects the temporal nature of cytokine secretion, with an essential role for TNFα in very early inflammation, whereas IL-6 is important during the transition from innate to adaptive immunity (for review see Jones, 2005). Our studies to date do not help define the location or nature of the cell surface sites to which IL-6 is delivered for release. Tracking fluorescently tagged IL-6 during its delivery to the plasma membrane has not yet revealed any particular feature or special sites for plasma membrane fusion. There may well be organization of IL-6 secretion sites at the level of membrane lipid microdomains, as there is for TNFα (Kay et al., 2006), or exocyst-demarked delivery sites, as seen on the apico-lateral membranes of epithelial cells (Yeaman et al., 2004; Rodriguez-Boulan et al., 2005). Interestingly, we also found that TfnR in recycling endosomes is not delivered to the actin-rich phagocytic cups. The cognate delivery of VAMP3 and TNFα to the cups and the concomitant exclusion of IL-6 and TfnR is evidence once again that sorting occurs in the recycling endosomes. Importantly, it shows that the recruitment of recycling endosome membrane for the formation of phagocytic cups at the cell surface occurs in a highly selective fashion, perhaps being designed to ensure that other trafficking and other cell functions can proceed unfettered by the onset of phagocytosis. It also highlights the temporal nature of phagosome maturation, a process that requires the sequential recruitment of different organelles in a SNARE-mediated fashion (Bajno et al., 2000; Collins et al., 2002; Braun et al., 2004). Although TfnR is excluded from early stage phagocytic cups, it can appear in more mature phagosomes (Clemens and Horwitz, 1995), suggesting that the recycling endosome plays a dynamic and evolving role throughout the phagocytic process.

In conclusion, the results shown in this study demonstrate the differential trafficking and secretion of cytokines from activated macrophages. Aspects of the post-Golgi trafficking that are shared or not shared by IL-6 and TNFα may suggest strategies for the joint or separate therapeutic targeting of these cytokines in inflammatory disease. A new route is demonstrated for IL-6 trafficking, one including recycling endosomes as a way station and possible sorting site. Our studies suggest that

mechanistically, sorting and compartmentalization of cargo within the macrophage recycling endosome enables the differential secretion of these proinflammatory cytokines and helps orchestrate the immune response.

Materials and methods

Antibodies and reagents

The following primary antibodies were used: rabbit polyclonal antibody to mouse IL-6 (Serotec), rabbit polyclonal and rat monoclonal anti–mouse TNFα antibodies (Calbiochem and Auspep, respectively), monoclonal antibodies to Stx6 and Vti1b (Translabs; BD Biosciences), monoclonal antibody to TfnR (Zymed Laboratories and Invitrogen), and a polyclonal rabbit antibody to VAMP3 (Abcam). Secondary antibodies used for immunofluorescence microscopy include Cy3-conjugated sheep anti–mouse IgG, Cy3-conjugated goat anti–rat IgG, and Cy3-conjugated goat anti–rabbit IgG, which were all purchased from Jackson ImmunoResearch Laboratories, as well as AlexaFluor488-conjugated goat anti–rat IgG and AlexaFluor647-conjugated goat anti–mouse IgG, which were both purchased from Invitrogen. Tetramethylrhodamine- and AlexaFluor647-conjugated Tfn and the $DiIC_{18}$(5)-DS lipophilic dye were purchased from Invitrogen. LPS from *Escherichia coli* serotype 0111:B4 was purchased from Sigma-Aldrich. IFNγ was purchased from R&D Systems.

Cell culture and transfection

RAW264.7 murine macrophages were cultured in RPMI 1640 medium (BioWhittaker) containing 10% heat-inactivated Serum Supreme (BioWhittaker) and 1% L-glutamine (Invitrogen) as previously described (Shurety et al., 2000). Macrophages were activated by the addition of 100–1,000 ng/ml LPS or 500 pg/ml IFNγ/LPS.

Full-length constructs of M6PR, TNFα, and the SNAREs Stx2, Stx6, VAMP3, and Vti1b were cloned into the pEGF-C1 vector (CLONTECH Laboratories, Inc., and BD Biosciences) to produce an N-terminal GFP-tagged protein as previously described (Murray et al., 2005a). TNFα and VAMP3 were also cloned into the pCherry-C1 vector (provided by R.Y. Tsien, University of California, San Diego, La Jolla, CA). IL-6 was cloned into the pGFP-N1 vector and the pCherry-N1 vector (adapted from the pCherry-C1 vector) to produce proteins that were C terminal tagged with either GFP or mCherry, respectively.

Macrophages were transfected for the transient expression of cDNAs by either electroporation or LipofectAMINE 2000 (Invitrogen). For electroporation, using an electroporation system (Gene Pulser II; Bio-Rad Laboratories), 2.5×10^7 cells were mixed with 10 μg DNA with a high capacitance setting (280 mV and 950 μF). Cells were then washed and typically cultured for 2–24 h before stimulation and/or imaging. For transfection with LipofectAMINE 2000, 15 μl of the reagent was mixed with 4 μg DNA in Opti-MEM (Invitrogen) per P6 plate containing 2×10^7 adherent cells. After 2 h, the cells were washed and further cultured for at least 1 h in complete medium before stimulation/imaging.

Tfn and lipophilic dye uptake

To label the recycling endosome, RAW264.7 cells were incubated with 10 μg/ml AlexaFluor647-conjugated Tfn in media for 15–60 min at 37°C before fixation in 4% PFA. Alternatively, cells were washed twice in serum-free media before the addition of 1 μM of the $DiIC_{18}$(5)-DS lipophilic dye, diluted in Opti-MEM (Invitrogen), and incubated for 5 min at 37°C followed by 15 min on ice. Unbound dye was removed by washing the cells three times in complete media before the addition of 10 μg/ml tetramethylrhodamine-conjugated Tfn in media and incubation for 20 min at 37°C. Finally, cells were washed before fixation in 4% PFA.

Assays for measuring IL-6 and TNFα production and secretion

The trafficking of TNFα and IL-6 from the Golgi complex to the cell surface was measured using an immunofluorescence-based assay. In brief, macrophages were incubated in the presence of 100 ng/ml LPS or 500 pg/ml IFN/100 ng/ml LPS for 4–6 h, fixed in 4% PFA, permeabilized with 0.1% Triton X-100, and stained by immunofluorescence for cell surface and intracellular TNFα (as previously described; Murray et al., 2005a) and IL-6. In some experiments, 5 μg/ml brefeldin A was added to the macrophages for the final 2 h of incubation. To determine the levels of secreted TNFα and IL-6, commercial ELISA kits (BD OptEIA; BD Biosciences) were used according to the manufacturer's instructions. In addition, to determine the levels of total IL-6 and TNFα within activated macrophages, cell lysates were prepared at the end of each time point and analyzed by Western blotting as described in Preparation of cell lysates, SDS-PAGE, and Western blotting.

Phagocytosis assays

In some experiments, macrophages were primed for 18 h in the presence of 500 pg/ml IFNγ before their incubation with live *Candida albicans* (at a ratio of 10 yeast per macrophage). Plates were briefly spun at 50 *g* for 2 min to encourage yeast–macrophage interactions, and a chase period of 5–20 min was performed at 37°C to allow phagocytosis to proceed. For live cell imaging, IgG-opsonized beads were added directly to the media immersing the imaging macrophages, and the videos were collected for up to a further 30 min.

Preparation of cell lysates, SDS-PAGE, and Western blotting

RAW264.7 cells were washed three times with PBS and lysed in buffer A (10 mM Tris, pH 7.4, containing 1 mM EDTA, 0.5% Triton X-100, and Complete protease inhibitors [Roche]). Cells were harvested by scraping followed by disruption via passaging through a series of successively smaller needles and centrifuged for 10 min at 17,000 *g*. The supernatant was assayed for protein content (Bio-Rad Laboratories protein assay), and 20–50 μg of total protein from each sample was subjected to SDS-PAGE separation and analyzed by immunoblotting.

Indirect immunofluorescence and live cell epifluorescence imaging

For indirect immunofluorescence, RAW264.7 cells were grown on glass coverslips before fixation in 1–4% PFA for 90 min. After fixation, the coverslips were washed in PBS and, if required, were permeabilized in 0.1% Triton X-100 for 5 min. Cells were then stained with appropriate primary and secondary antibodies before mounting in 50% glycerol containing 1,4-dazabiccyclo-2,2,2-octane (Sigma-Aldrich). Epifluorescence still images were captured on an inverted microscope (IX71; Olympus) with a 100× oil objective and a 12-bit 1,280 × 1,024-pixel CCD camera (IMAGO Super VGA; TILL Photonics). Confocal images were captured on a microscope (LSM510 META; Carl Zeiss MicroImaging, Inc.) using optical spectral separation or digital emission fingerprinting. Single images were captured with an optical thickness of 0.7–1.7 μm, and, for z series, a 0.34–0.7-μm step interval was used. Analysis was performed using LSM510 META software (Carl Zeiss MicroImaging, Inc.) and Photoshop CS2 (Adobe). For 3D reconstructions, the area of interest was extracted, and each cargo was surface rendered using the LSM510 META software. The thresholds for the fluorescent intensity of each channel were carefully adjusted to most closely represent the signal strength of the original 2D images collected.

For live cell experiments, cells were cultured on 25-mm round glass coverslips or in glass-bottom 35-mm dishes (MatTek Corporation). Live cell epifluorescence imaging was performed using inverted microscopes (IX71 or IX81; Olympus). Coverslips were mounted in a temperature-controlled heating block, warmed to 37°C, and maintained to within ±0.2°C using a heated water bath or with cells in MatTek dishes maintained at 37°C by use of a microscope incubator (Solvent Scientific). In both cases, the cells were incubated in CO_2-independent medium containing 10% heat-inactivated FCS (Lock et al., 2005). Fluorophore excitation was achieved with a Xenon lamp-based monochromatic light generator (Polychrome IV; TILL Photonics) controlled by a digital signal processor board (TILL Photonics) on the IX71 microscope and an illumination system (MT20; Olympus) on the IX81 microscope. Images were captured through either a UPlanSApo 60×/NA 1.35 or 100×/NA 1.40 oil objective (Olympus). A 12-bit 1,280 × 1,024-pixel camera (IMAGO Super VGA; TILL Photonics) was used to capture the images on the IX71 microscope, and a 12-bit 1,376 × 1,032-pixel high resolution camera (F-VIEW; Olympus) was used on the IX81 inverted microscope. For single-color videos, frame capture rates were between 200 and 2,000 ms, with total capture periods ranging from 2 to 45 min. For dual-color videos, individual channels were captured sequentially, with typical capture rates of 100–1,000 ms for GFP and capture rates of 80–400 ms for mCherry. Importantly, the GFP signal was captured first, followed by mCherry. Image control and postcapture image analysis were performed using either TILLVISION (TILL Photonics) or CellR v2.5 software (Olympus).

Videos were analyzed, cropped, and constructed using ImageJ v1.37p (National Institutes of Health), Volocity v3.7 (Improvision), Photoshop CS2 (Adobe), and TILLVISION software and were exported as QuickTime videos (Apple) with a playback speed of 10 frames per second. An additional ImageJ plugin, ParticleTracker, was used for automated detection and tracking of particles recorded by video imaging (Sbalzarini and Koumoutsakos, 2005). 200 frames were analyzed for each channel, the particle radius was set at two pixels, and the maximum pixel displacement allowed between frames for particles was two. The resulting detected

particles and their tracks were filtered so only those that were continuous for five or more frames were displayed on an overlay of the channel. Each detected track is shown at its full length as a continuous color, with red sections being interpolated by the plugin to handle occlusions (Sbalzarini and Koumoutsakos, 2005).

Golgi isolation and in vitro vesicle budding assay

A stacked Golgi membrane fraction and subsequent in vitro budded Golgi-derived vesicles were prepared from RAW264.7 cells stimulated with 100 ng/ml LPS for 6 h by density gradient centrifugation based on previously published methods (Heimann et al., 1999; Wylie et al., 1999). The resulting fractions were analyzed by SDS-PAGE and immunoblotting.

siRNA treatment

RAW264.7 cells plated on glass coverslips were subjected to two rounds of transfection of siRNA constructs using LipofectAMINE 2000 (Invitrogen) according to the manufacturer's instructions, each 24 h apart, and were finally cultured for a further 24 h before LPS stimulation. The following siRNAs were used in these experiments: scramble (siRNA ID# 4635), glyceraldehyde-3-phosphate dehydrogenase (ID# 4631), mouse VAMP3 (ID# 186990), Vti1b (ID# 184555), and Stx6 (ID#7 5897). All constructs were purchased from Ambion. Western blotting and immunofluorescence were used to confirm the knockdown of the target proteins.

Endosomal inactivation assay

An HRP inactivation assay was modified from the protocol of Ang et al. (2004) and as previously described (Futter et al., 1995; Murray et al., 2005a). In brief, RAW264.7 cells were incubated with 10 μg/ml Tfn-HRP in media for 30 min in the dark at 37°C. Cells were washed twice in ice-cold PBS, and surface-bound Tfn-HRP was removed by two 5-min washes with 0.15 M NaCl and 20 mM citric acid, pH 5. Cells were then washed twice with ice-cold PBS and incubated in the dark for 1 h with PBS containing 0.1 mg/ml DAB and 0.025% H_2O_2 to the inactivation sample (the control contained DAB but no H_2O_2). Cells were finally washed twice in PBS containing 1% BSA to stop the reaction and were incubated in prewarmed media containing 500 pg/ml IFN and 100 ng/ml LPS for 6 h at 37°C. Supernatant was collected after 2 h and 6 h to determine the level of TNFα and IL-6 secretion, respectively. Coverslips were fixed in 4% PFA and immunostained for internal TNFα and IL-6.

EM and immunogold labeling

Immuno-EM of ultrathin cryosections was performed as previously described (Brown et al., 2001). In brief, after fixation in 4% PFA (EM grade; ProSciTech), RAW264.7 cells were embedded in warm gelatin and frozen onto cryostubs. Ultra-thin cryosections were collected onto copper grids and immunolabeled according to Slot et al. (1991). Antibodies were detected with either different-sized protein A–gold conjugates (provided by J. Slot, University of Utrecht, Utrecht, Netherlands) or species-specific gold probes (British BioCell, Australian Laboratory Services). Sections were viewed on an electron microscope (model 1011; JEOL), whereas images were captured using the iTEM analysis program (Soft Imaging System).

Online supplemental material

Video 1 shows IL-6 exiting the Golgi in a budded vesicle. Video 2 shows IL-6 exiting the Golgi in vesicular and budded vesicles. Video 3 shows that IL-6 exits the TGN in carriers both with and without TNF. Video 4 shows IL-6 exiting the Golgi in a budded vesicle and fusing with the recycling endosome. Video 5 shows that IL-6 exits the recycling endosome without TNF. Video 6 shows that IL-6 does not traffic to the forming phagocytic cup. Online supplemental material is available at http://www.jcb.org/cgi/content/full/jcb.200612131/DC1.

We thank T. Khromykh, J. Venturato, and T. Munchow for assistance.

This work was supported by funding from the National Institutes of Health and by a fellowship and grant to J.L. Stow from the National Health and Medical Research Council of Australia.

Submitted: 22 December 2006
Accepted: 6 June 2007

References

Andersson, U., and T. Matsuda. 1989. Human interleukin 6 and tumor necrosis factor alpha production studied at a single-cell level. *Eur. J. Immunol.* 19:1157–1160.

Ang, A.L., T. Taguchi, S. Francis, H. Folsch, L.J. Murrells, M. Pypaert, G. Warren, and I. Mellman. 2004. Recycling endosomes can serve as intermediates during transport from the Golgi to the plasma membrane of MDCK cells. *J. Cell Biol.* 167:531–543.

Arvan, P., B.Y. Zhang, L. Feng, M. Liu, and R. Kuliawat. 2002. Lumenal protein multimerization in the distal secretory pathway/secretory granules. *Curr. Opin. Cell Biol.* 14:448–453.

Bajno, L., X.R. Peng, A.D. Schreiber, H.P. Moore, W.S. Trimble, and S. Grinstein. 2000. Focal exocytosis of VAMP3-containing vesicles at sites of phagosome formation. *J. Cell Biol.* 149:697–706.

Barton, B.E., and J.V. Jackson. 1993. Protective role of interleukin 6 in the lipopolysaccharide-galactosamine septic shock model. *Infect. Immun.* 61:1496–1499.

Beutler, B.A. 1999. The role of tumor necrosis factor in health and disease. *J. Rheumatol. Suppl.* 57:16–21.

Bonifacino, J.S., and R. Rojas. 2006. Retrograde transport from endosomes to the trans-Golgi network. *Nat. Rev. Mol. Cell Biol.* 7:568–579.

Braun, V., V. Fraisier, G. Raposo, I. Hurbain, J.B. Sibarita, P. Chavrier, T. Galli, and F. Niedergang. 2004. TI-VAMP/VAMP7 is required for optimal phagocytosis of opsonised particles in macrophages. *EMBO J.* 23:4166–4176.

Brown, D.L., K. Heimann, J. Lock, L. Kjer-Nielsen, C. van Vliet, J.L. Stow, and P.A. Gleeson. 2001. The GRIP domain is a specific targeting sequence for a population of trans-Golgi network derived tubulo-vesicular carriers. *Traffic*. 2:336–344.

Caplan, M.J., J.L. Stow, A.P. Newman, J. Madri, H.C. Anderson, M.G. Farquhar, G.E. Palade, and J.D. Jamieson. 1987. Dependence on pH of polarized sorting of secreted proteins. *Nature*. 329:632–635.

Casanova, J.E., X. Wang, R. Kumar, S.G. Bhartur, J. Navarre, J.E. Woodrum, Y. Altschuler, G.S. Ray, and J.R. Goldenring. 1999. Association of Rab25 and Rab11a with the apical recycling system of polarized Madin-Darby canine kidney cells. *Mol. Biol. Cell*. 10:47–61.

Clemens, D.L., and M.A. Horwitz. 1995. Characterization of the Mycobacterium tuberculosis phagosome and evidence that phagosomal maturation is inhibited. *J. Exp. Med.* 181:257–270.

Collins, R.F., A.D. Schreiber, S. Grinstein, and W.S. Trimble. 2002. Syntaxins 13 and 7 function at distinct steps during phagocytosis. *J. Immunol.* 169:3250–3256.

Cox, D., D.J. Lee, B.M. Dale, J. Calafat, and S. Greenberg. 2000. A Rab11-containing rapidly recycling compartment in macrophages that promotes phagocytosis. *Proc. Natl. Acad. Sci. USA*. 97:680–685.

Daro, E., P. van der Sluijs, T. Galli, and I. Mellman. 1996. Rab4 and cellubrevin define different early endosome populations on the pathway of transferrin receptor recycling. *Proc. Natl. Acad. Sci. USA*. 93:9559–9564.

Ellis, M.A., B.A. Potter, K.O. Cresawn, and O.A. Weisz. 2006. Polarized biosynthetic traffic in renal epithelial cells: sorting, sorting, everywhere. *Am. J. Physiol. Renal Physiol.* 291:F707–F713.

Futter, C.E., C.N. Connolly, D.F. Cutler, and C.R. Hopkins. 1995. Newly synthesized transferrin receptors can be detected in the endosome before they appear on the cell surface. *J. Biol. Chem.* 270:10999–11003.

Gagescu, R., N. Demaurex, R.G. Parton, W. Hunziker, L.A. Huber, and J. Gruenberg. 2000. The recycling endosome of Madin-Darby canine kidney cells is a mildly acidic compartment rich in raft components. *Mol. Biol. Cell*. 11:2775–2791.

Ghosh, P., N.M. Dahms, and S. Kornfeld. 2003. Mannose 6-phosphate receptors: new twists in the tale. *Nat. Rev. Mol. Cell Biol.* 4:202–212.

Heimann, K., J.M. Percival, R. Weinberger, P. Gunning, and J.L. Stow. 1999. Specific isoforms of actin-binding proteins on distinct populations of Golgi-derived vesicles. *J. Biol. Chem.* 274:10743–10750.

Hurst, S.M., T.S. Wilkinson, R.M. McLoughlin, S. Jones, S. Horiuchi, N. Yamamoto, S. Rose-John, G.M. Fuller, N. Topley, and S.A. Jones. 2001. Il-6 and its soluble receptor orchestrate a temporal switch in the pattern of leukocyte recruitment seen during acute inflammation. *Immunity*. 14:705–714.

Huse, M., B.F. Lillemeier, M.S. Kuhns, D.S. Chen, and M.M. Davis. 2006. T cells use two directionally distinct pathways for cytokine secretion. *Nat. Immunol.* 7:247–255.

Jin, M., and J.R. Goldenring. 2006. The Rab11-FIP1/RCP gene codes for multiple protein transcripts related to the plasma membrane recycling system. *Biochim. Biophys. Acta*. 1759:281–295.

Jones, S.A. 2005. Directing transition from innate to acquired immunity: defining a role for IL-6. *J. Immunol.* 175:3463–3468.

Kandere-Grzybowska, K., R. Letourneau, D. Kempuraj, J. Donelan, S. Poplawski, W. Boucher, A. Athanassiou, and T.C. Theoharides. 2003. IL-1 induces vesicular secretion of IL-6 without degranulation from human mast cells. *J. Immunol.* 171:4830–4836.

Kay, J.G., R.Z. Murray, J.K. Pagan, and J.L. Stow. 2006. Cytokine secretion via cholesterol-rich lipid raft-associated SNAREs at the phagocytic cup. *J. Biol. Chem.* 281:11949–11954.

Kim, T., J.H. Tao-Cheng, L.E. Eiden, and Y.P. Loh. 2001. Chromogranin A, an "on/off" switch controlling dense-core secretory granule biogenesis. *Cell*. 106:499–509.

Kishimoto, T., S. Akira, M. Narazaki, and T. Taga. 1995. Interleukin-6 family of cytokines and gp130. *Blood*. 86:1243–1254.

Kracht, M., and J. Saklatvala. 2002. Transcriptional and post-transcriptional control of gene expression in inflammation. *Cytokine*. 20:91–106.

Kwak, D.J., N.H. Augustine, W.G. Borges, J.L. Joyner, W.F. Green, and H.R. Hill. 2000. Intracellular and extracellular cytokine production by human mixed mononuclear cells in response to group B streptococci. *Infect. Immun.* 68:320–327.

Lapierre, L.A., and J.R. Goldenring. 2005. Interactions of myosin vb with rab11 family members and cargoes traversing the plasma membrane recycling system. *Methods Enzymol.* 403:715–723.

Lapierre, L.A., M.C. Dorn, C.F. Zimmerman, J. Navarre, J.O. Burnette, and J.R. Goldenring. 2003. Rab11b resides in a vesicular compartment distinct from Rab11a in parietal cells and other epithelial cells. *Exp. Cell Res.* 290:322–331.

Lock, J.G., and J.L. Stow. 2005. Rab11 in recycling endosomes regulates the sorting and basolateral transport of E-cadherin. *Mol. Biol. Cell*. 16:1744–1755.

Lock, J.G., L.A. Hammond, F. Houghton, P.A. Gleeson, and J.L. Stow. 2005. E-cadherin transport from the trans-Golgi network in tubulovesicular carriers is selectively regulated by golgin-97. *Traffic*. 6:1142–1156.

Meyers, J.M., and R. Prekeris. 2002. Formation of mutually exclusive Rab11 complexes with members of the family of Rab11-interacting proteins regulates Rab11 endocytic targeting and function. *J. Biol. Chem.* 277:49003–49010.

Moqbel, R., and J.J. Coughlin. 2006. Differential secretion of cytokines. *Sci. STKE*. doi:10.1126/stke.3382006pe26.

Murray, R.Z., J.G. Kay, D.G. Sangermani, and J.L. Stow. 2005a. A role for the phagosome in cytokine secretion. *Science*. 310:1492–1495.

Murray, R.Z., F.G. Wylie, T. Khromykh, D.A. Hume, and J.L. Stow. 2005b. Syntaxin 6 and Vti1b form a novel SNARE complex, which is up-regulated in activated macrophages to facilitate exocytosis of tumor necrosis Factor-alpha. *J. Biol. Chem.* 280:10478–10483.

Nishimoto, N., and T. Kishimoto. 2004. Inhibition of IL-6 for the treatment of inflammatory diseases. *Curr. Opin. Pharmacol.* 4:386–391.

Orzech, E., S. Cohen, A. Weiss, and B. Aroeti. 2000. Interactions between the exocytic and endocytic pathways in polarized Madin-Darby canine kidney cells. *J. Biol. Chem.* 275:15207–15219.

Pagan, J.K., F.G. Wylie, S. Joseph, C. Widberg, N.J. Bryant, D.E. James, and J.L. Stow. 2003. The t-SNARE syntaxin 4 is regulated during macrophage activation to function in membrane traffic and cytokine secretion. *Curr. Biol.* 13:156–160.

Polishchuk, R.S., E.V. Polishchuk, P. Marra, S. Alberti, R. Buccione, A. Luini, and A.A. Mironov. 2000. Correlative light-electron microscopy reveals the tubular-saccular ultrastructure of carriers operating between Golgi apparatus and plasma membrane. *J. Cell Biol.* 148:45–58.

Polishchuk, R.S., E. San Pietro, A. Di Pentima, S. Tete, and J.S. Bonifacino. 2006. Ultrastructure of long-range transport carriers moving from the trans Golgi network to peripheral endosomes. *Traffic*. 7:1092–1103.

Powelka, A.M., J. Sun, J. Li, M. Gao, L.M. Shaw, A. Sonnenberg, and V.W. Hsu. 2004. Stimulation-dependent recycling of integrin beta1 regulated by ARF6 and Rab11. *Traffic*. 5:20–36.

Rodriguez-Boulan, E., and A. Musch. 2005. Protein sorting in the Golgi complex: shifting paradigms. *Biochim. Biophys. Acta*. 1744:455–464.

Rodriguez-Boulan, E., G. Kreitzer, and A. Musch. 2005. Organization of vesicular trafficking in epithelia. *Nat. Rev. Mol. Cell Biol.* 6:233–247.

Sbalzarini, I.F., and P. Koumoutsakos. 2005. Feature point tracking and trajectory analysis for video imaging in cell biology. *J. Struct. Biol.* 151:182–195.

Schlierf, B., G.H. Fey, J. Hauber, G.M. Hocke, and O. Rosorius. 2000. Rab11b is essential for recycling of transferrin to the plasma membrane. *Exp. Cell Res.* 259:257–265.

Shurety, W., A. Merino-Trigo, D. Brown, D.A. Hume, and J.L. Stow. 2000. Localization and post-Golgi trafficking of tumor necrosis factor-alpha in macrophages. *J. Interferon Cytokine Res.* 20:427–438.

Siddiqui, M.A., and L.J. Scott. 2005. Infliximab: a review of its use in Crohn's disease and rheumatoid arthritis. *Drugs*. 65:2179–2208.

Slot, J.W., H.J. Geuze, S. Gigengack, G.E. Lienhard, and D.E. James. 1991. Immuno-localization of the insulin regulatable glucose transporter in brown adipose tissue of the rat. *J. Cell Biol.* 113:123–135.

Sonnichsen, B., S. De Renzis, E. Nielsen, J. Rietdorf, and M. Zerial. 2000. Distinct membrane domains on endosomes in the recycling pathway visualized by multicolor imaging of Rab4, Rab5, and Rab11. *J. Cell Biol.* 149:901–914.

Spencer, L.A., R.C. Melo, S.A. Perez, S.P. Bafford, A.M. Dvorak, and P.F. Weller. 2006. Cytokine receptor-mediated trafficking of preformed IL-4 in eosinophils identifies an innate immune mechanism of cytokine secretion. *Proc. Natl. Acad. Sci. USA*. 103:3333–3338.

Teter, K., G. Chandy, B. Quinones, K. Pereyra, T. Machen, and H.P. Moore. 1998. Cellubrevin-targeted fluorescence uncovers heterogeneity in the recycling endosomes. *J. Biol. Chem.* 273:19625–19633.

Trowbridge, I.S., J.F. Collawn, and C.R. Hopkins. 1993. Signal-dependent membrane protein trafficking in the endocytic pathway. *Annu. Rev. Cell Biol.* 9:129–161.

Ulich, T.R., S. Yin, K. Guo, E.S. Yi, D. Remick, and J. del Castillo. 1991. Intratracheal injection of endotoxin and cytokines. II. Interleukin-6 and transforming growth factor beta inhibit acute inflammation. *Am. J. Pathol.* 138:1097–1101.

Ullrich, O., S. Reinsch, S. Urbe, M. Zerial, and R.G. Parton. 1996. Rab11 regulates recycling through the pericentriolar recycling endosome. *J. Cell Biol.* 135:913–924.

van Ijzendoorn, S.C. 2006. Recycling endosomes. *J. Cell Sci.* 119:1679–1681.

Wylie, F., K. Heimann, T.L. Le, D. Brown, G. Rabnott, and J.L. Stow. 1999. GAIP, a Galphai-3-binding protein, is associated with Golgi-derived vesicles and protein trafficking. *Am. J. Physiol.* 276:C497–C506.

Yeaman, C., K.K. Grindstaff, and W.J. Nelson. 2004. Mechanism of recruiting Sec6/8 (exocyst) complex to the apical junctional complex during polarization of epithelial cells. *J. Cell Sci.* 117:559–570.